

# Telmisartan Improves Insulin Resistance of Skeletal Muscle Through Peroxisome Proliferator-Activated Receptor- $\delta$ Activation

Li Li, Zhidan Luo, Hao Yu, Xiaoli Feng, Peijian Wang, Jian Chen, Yunfei Pu, Yu Zhao, Hongbo He, Jian Zhong, Daoyan Liu, and Zhiming Zhu

The mechanisms of the improvement of glucose homeostasis through angiotensin receptor blockers are not fully elucidated in hypertensive patients. We investigated the effects of telmisartan on insulin signaling and glucose uptake in cultured myotubes and skeletal muscle from wild-type and muscle-specific peroxisome proliferator-activated receptor (PPAR)  $\delta$  knockout (MCK-PPAR $\delta^{-/-}$ ) mice. Telmisartan increased PPAR $\delta$  expression and activated PPAR $\delta$  transcriptional activity in cultured C2C12 myotubes. In palmitate-induced insulin-resistant C2C12 myotubes, telmisartan enhanced insulin-stimulated Akt and Akt substrate of 160 kDa (AS160) phosphorylation as well as Glut4 translocation to the plasma membrane. These effects were inhibited by antagonizing PPAR $\delta$  or phosphatidylinositol-3 kinase, but not by PPAR $\gamma$  and PPAR $\alpha$  inhibition. Palmitate reducing the insulin-stimulated glucose uptake in C2C12 myotubes could be restored by telmisartan. In vivo experiments showed that telmisartan treatment reversed high-fat diet-induced insulin resistance and glucose intolerance in wild-type mice but not in MCK-PPAR $\delta^{-/-}$  mice. The protein levels of PPAR $\delta$ , phospho-Akt, phospho-AS160, and Glut4 translocation to the plasma membrane in the skeletal muscle on insulin stimulation were reduced by high-fat diet and were restored by telmisartan administration in wild-type mice. These effects were absent in MCK-PPAR $\delta^{-/-}$  mice. These findings implicate PPAR $\delta$  as a potential therapeutic target in the treatment of hypertensive subjects with insulin resistance. *Diabetes* 62:762–774, 2013

**T**he underlying metabolic causes of type 2 diabetes are the combination of insulin resistance and defective secretion of insulin by pancreatic  $\beta$ -cells. Insulin resistance typically precedes the onset of type 2 diabetes (1) and is commonly accompanied by other cardiovascular risk factors, such as dyslipidemia, hypertension, and metabolic syndrome (2). Several large clinical trials demonstrate that angiotensin-converting enzyme inhibitors or angiotensin II receptor blockers (ARBs) can significantly reduce the incidence of new cases of type 2 diabetes in patients at high risk compared with other antihypertensive therapies (3). However, the mechanisms

involved in improved glucose homeostasis through ARBs are not completely understood.

Several recent studies show that ARBs exert beneficial effects on lipid and glucose metabolism that involve more than just their ability to block the angiotensin II receptor (2). These may include enhancing blood flow through the microcirculation of skeletal muscle (4) and increasing plasma adiponectin concentration (5). In addition, several ARBs, including telmisartan (TM), have been found to effectively activate the peroxisome proliferator-activated receptor (PPAR)  $\gamma$  (6,7). PPAR isoforms display tissue-specific expression and gene-regulatory profiles. PPAR $\gamma$  is a key regulator of adipocyte differentiation and adipose insulin sensitivity (8,9), but it is expressed at extremely low levels, if at all, in skeletal muscle. In contrast, PPAR $\delta$  (also referred to as PPAR $\beta$ ) is expressed in a wide variety of tissues, with high levels in skeletal muscle (10). Recent studies show a crucial role of PPAR $\delta$  in skeletal muscle glucose metabolism and insulin action. Krämer et al. (11) showed that activation of PPAR $\delta$  results in a direct increase of fatty acid transport and glucose uptake and promotes lipid and glucose metabolism and gene expression in primary cultured human skeletal muscle cells (12,13). Muscle-specific PPAR $\delta$ -transgenic mice were used to establish the role of PPAR $\delta$  in whole-body glucose homeostasis. Schuler et al. (14) showed that mice in which PPAR $\delta$  is selectively ablated in skeletal muscle myocytes exhibit fiber-type switching, obesity, and type 2 diabetes, demonstrating that PPAR $\delta$  is instrumental for peripheral insulin sensitivity.

The PPAR $\delta$ -specific agonist GW501516 improves glucose tolerance and reduces plasma glucose and insulin levels in several animal models (15,16). Therefore, activation of PPAR $\delta$  may offer an effective strategy to improve glucose homeostasis. However, the safety issues about this pharmacological agonist are still highly controversial (17,18). Thus, it is important to know whether ARBs, such as TM, affect PPAR $\delta$  activity. Given the importance of skeletal muscle insulin resistance in the development of type 2 diabetes, we hypothesized that TM may affect glucose metabolism in skeletal muscle by activating PPAR $\delta$ . Here, we present evidences supporting that TM as a bona fide ligand of PPAR $\delta$  and its activation on phosphatidylinositol 3-kinase (PI3K) pathway are key mechanisms of enhancing insulin sensitivity and glucose uptake in skeletal muscle.

## RESEARCH DESIGN AND METHODS

**Materials.** TM, palmitate, PPAR $\gamma$  inhibitor GW9662, PPAR $\delta$  inhibitor GSK0660, PPAR $\alpha$  inhibitor GW6471, and PI3K inhibitor LY294002 were all purchased from Sigma-Aldrich (St. Louis, MO).

**Generation of muscle-specific PPAR $\delta$  knockout mice.** Transgenic mice having the Cre recombinase gene driven by the muscle creatine kinase (MCK-Cre)

From the Center for Hypertension and Metabolic Diseases, Department of Hypertension and Endocrinology, Daping Hospital, Third Military Medical University, Chongqing Institute of Hypertension, Chongqing, China.

Corresponding author: Zhiming Zhu, zhuzm@yahoo.com, or Daoyan Liu, daoyanliu@yahoo.com.

Received 2 May 2012 and accepted 13 September 2012.

DOI: 10.2337/db12-0570

This article contains Supplementary Data online at <http://diabetes.diabetesjournals.org/lookup/suppl/doi:10.2337/db12-0570/-/DC1>.

L.L. and Z.L. contributed equally to this study.

© 2013 by the American Diabetes Association. Readers may use this article as long as the work is properly cited, the use is educational and not for profit, and the work is not altered. See <http://creativecommons.org/licenses/by-nc-nd/3.0/> for details.

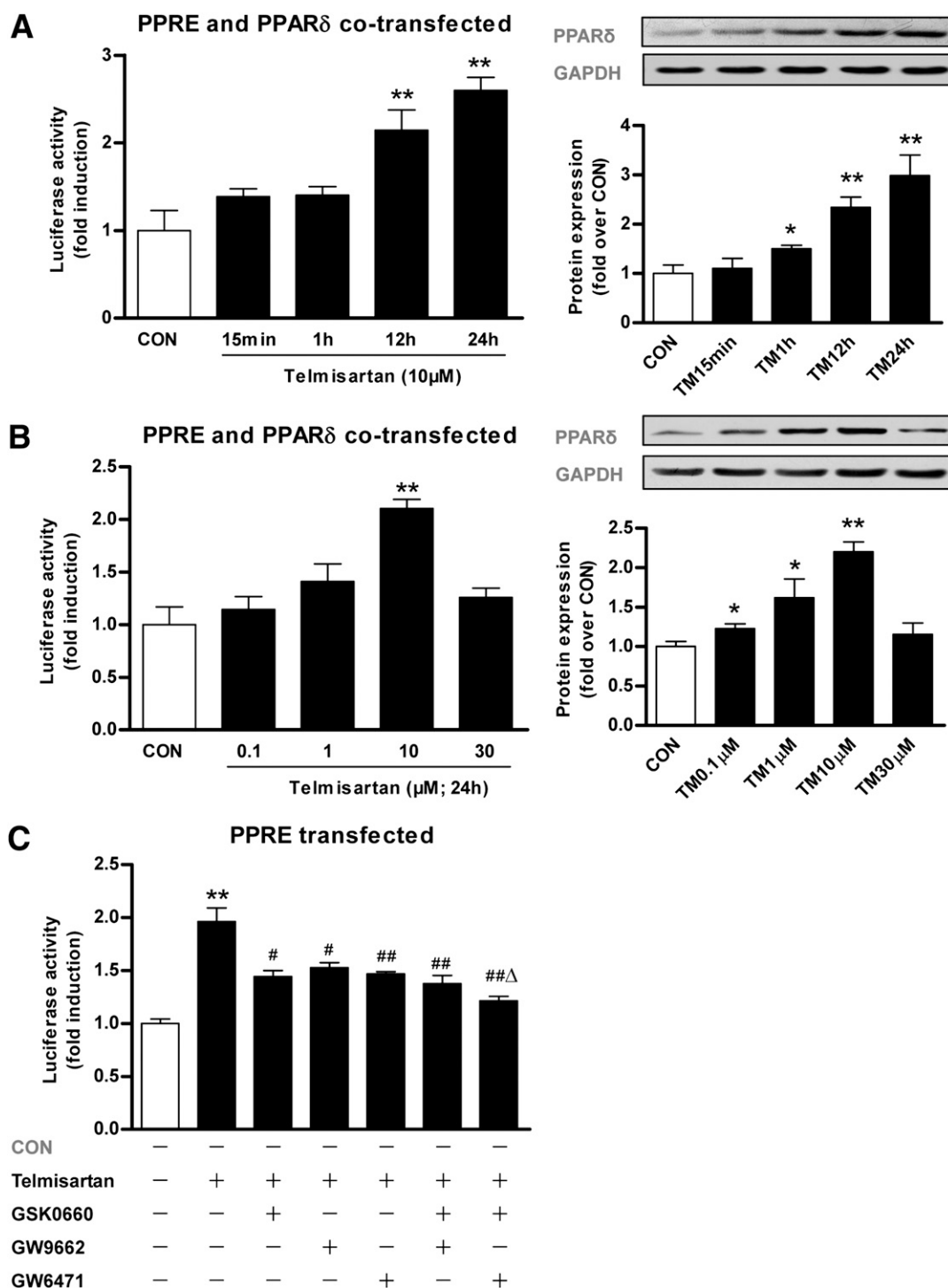


**FIG. 1.** Effect of TM on PPAR $\delta$  expression and activity in C2C12 myotubes. **A:** PPRE activity in C2C12 myotubes transfected with pTK-PPREx3-luc was evaluated by luciferase assay. PPAR $\delta$  expression in C2C12 myotubes transfected with pTK-PPREx3-luc was detected by Western blotting. C2C12 myotubes with cotransfection the plasmid pAdTrack-CMV-PPAR- $\delta$ , containing the full-length coding region of rat PPAR $\delta$  (PPAR $\delta$  vector), were treated with DMSO (control [CON]) or TM (10  $\mu$ mol/L) for 15 min to 24 h before the luciferase assay or Western blotting. \* $P$  < 0.05 and \*\* $P$  < 0.01 vs. CON. **B:** PPRE activity in C2C12 myotubes cotransfected with pTK-PPREx3-luc and PPAR $\delta$  vector was evaluated by luciferase assay. PPAR $\delta$  expression in C2C12 myotubes transfected with pTK-PPREx3-luc was detected by Western blotting. Cells were treated with DMSO (CON) or indicated concentrations of TM (0.1–30  $\mu$ mol/L) for 24 h. \* $P$  < 0.05 and \*\* $P$  < 0.01 vs. CON. **C:** Cells were treated with DMSO (CON) or 10  $\mu$ mol/L TM for 24 h. Cells were treated with 10  $\mu$ mol/L TM in the presence or absence of PPAR $\delta$  inhibitor GSK0660 (GSK; 10  $\mu$ mol/L), PPAR $\gamma$  inhibitor GW9662 (GW9662; 10  $\mu$ mol/L), or PPAR $\alpha$  inhibitor GW6471 (GW6471; 10  $\mu$ mol/L) for 24 h before the luciferase assay. \*\* $P$  < 0.01 vs. CON; # $P$  < 0.05 and ## $P$  < 0.01 vs. TM 10  $\mu$ mol/L;  $\Delta$  $P$  < 0.05 vs. TM 10  $\mu$ mol/L plus GSK 10  $\mu$ mol/L. **D:** 10  $\mu$ mol/L TM treatment for 24 h increased the luciferase activity both in an empty pAdTrack expression vector as the control and the cotransfection with the PPAR $\delta$  expression vector in transfected C2C12 myotubes. \* $P$  < 0.05 and \*\* $P$  < 0.01 versus CON; # $P$  < 0.05 vs. PPAR $\delta$  vector plus TM 10  $\mu$ mol/L. **E:** PPAR $\delta$ , PPAR $\gamma$ , and PPAR $\alpha$  expression in C2C12 myotubes was detected by Western blotting after treatment with DMSO (CON) or TM (10  $\mu$ mol/L) for 24 h. \* $P$  < 0.05 vs. CON. Data are mean  $\pm$  SEM from 3–6 experiments.

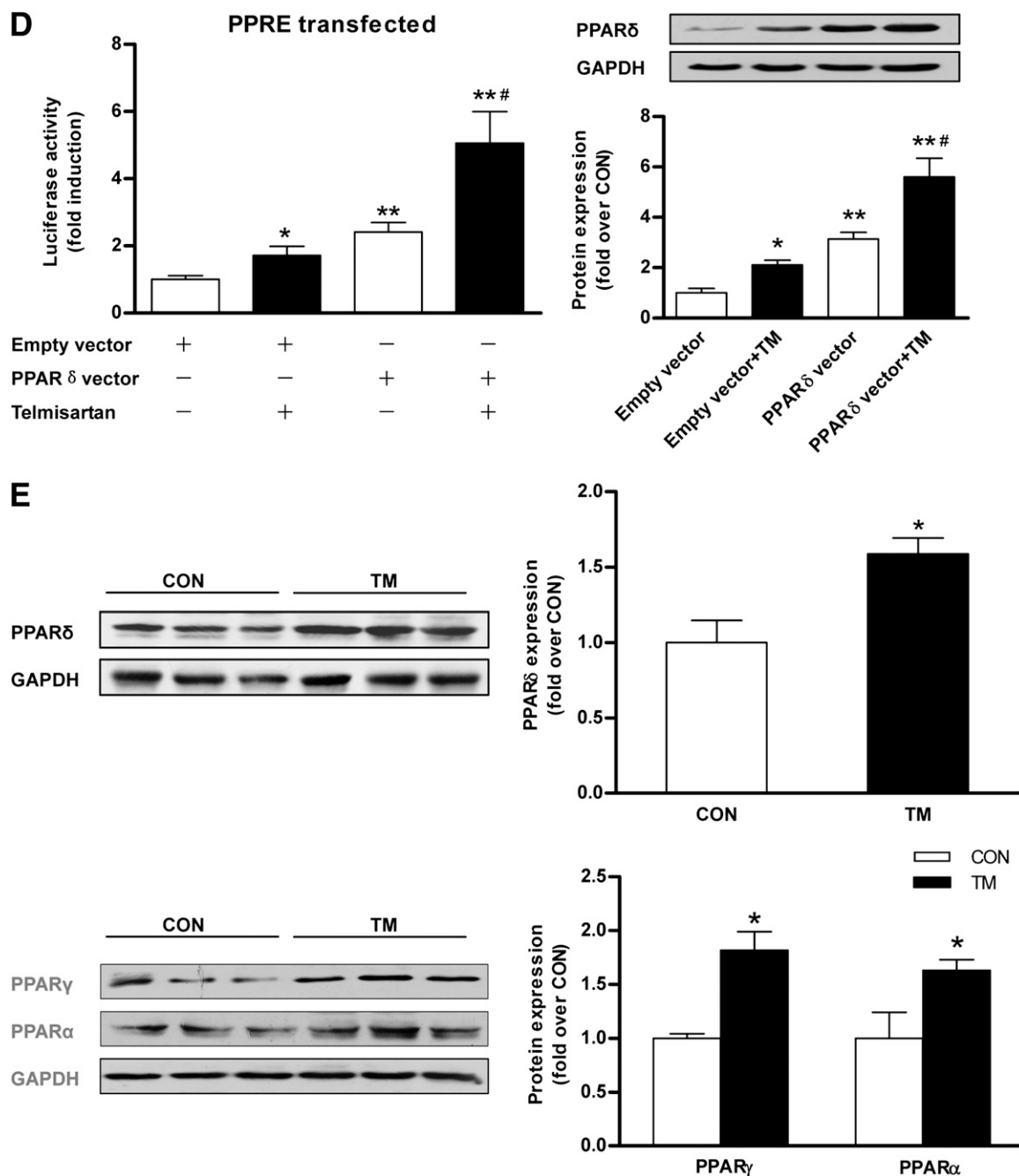
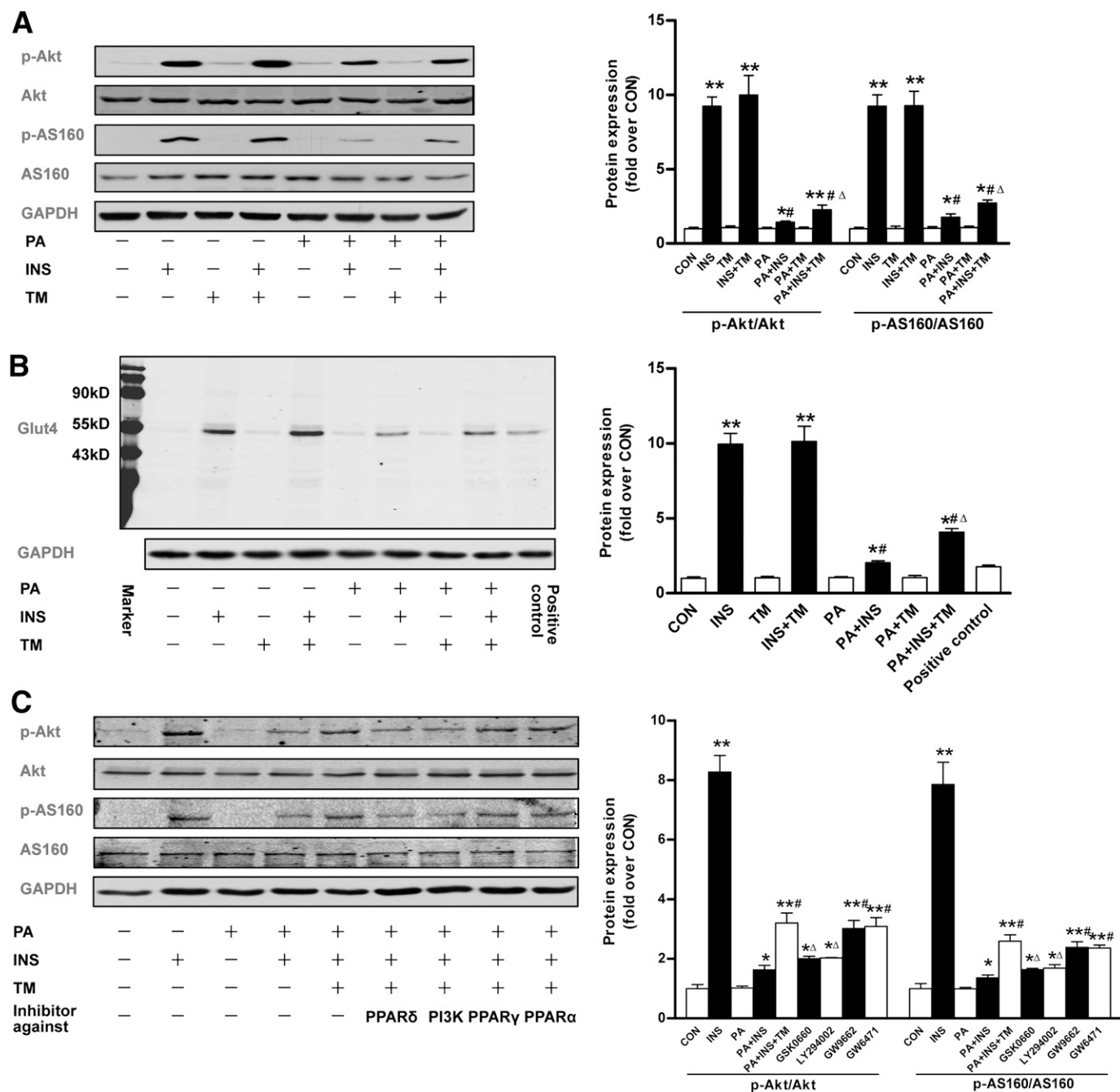


FIG. 1. Continued.

promoter were purchased from The Jackson Laboratory (stock number 006475). Cre activity is observed in skeletal muscle. Mice possess loxP sites on either side of exon 4 of PPAR $\delta$  gene (PPAR $\delta^{lox/lox}$ ) were also purchased from The Jackson Laboratory (stock number 005897). Mice with hemizygous MCK-Cre and homozygous PPAR $\delta^{lox}$  allele are viable, fertile, and normal in size. Breeding of these two types of mice yielded Cre:PPAR $\delta^{lox/+}$  mice. Then, breeding of Cre:PPAR $\delta^{lox/+}$  mice with PPAR $\delta^{lox/lox}$  mice yielded Cre:PPAR $\delta^{lox/lox}$  mice, which have PPAR $\delta$ -specific knockout in skeletal muscles (MCK-PPAR $\delta^{-/-}$ ). The PPAR $\delta^{lox/lox}$  littermates were used as control mice (wild-type [WT]) (19). DNA prepared from tail biopsy samples was used for genotyping by PCR using the following primers: for MCK-Cre, 5'-GTG AAA CAG CAT TGC TGT CAC TT-3' (primer 1) and 5'-TAA GTC TGA ACC CGG TCT GC-3' (primer 2) were used; and for PPAR $\delta^{lox}$ , 5'-GAG CCG CCT CTC GCC ATC CTT TCA G-3' (primer 1), 5'-GGC GTG GGG ATT TGC CTG CTT CA-3' (primer 2), and 5'-GTC GAG AAG TAC TAG TGG CCA CGT GG-3' (primer 3) were used. **Animals and experimental procedure.** Mice were housed in cages at a controlled temperature (22  $\pm$  1°C) and relative humidity (55  $\pm$  15%) in a 12-h light/12-h dark cycle. They were supplied with standard laboratory chow and

tap water ad libitum until 6 weeks of age. Then, a high-fat diet (HFD) was supplied for 20 weeks to induce insulin resistance in the mice (20). After undergoing intraperitoneal glucose tolerance test (IPGTT) and intraperitoneal insulin tolerance test (IPITT), the mice were randomly given normal chow diet or HFD without (control or high-fat [HF] group,  $n = 6$ ) or with TM (TM group or HF+TM group,  $n = 6$ ) for another 10 weeks. TM (5 mg/kg body weight) was administrated by mixing into the normal chow diet or HFD. The mice kept on regular rodent chow were considered the control (control group,  $n = 6$ ) throughout the experiment. The food intake was measured every day. Body weights were measured every 2 weeks. At the end of experiment, the mice were subjected to IPGTT and IPITT again. Then, the mice were killed after fasting for 14 h. The gastrocnemius muscle was removed and stored at -70°C for Western blot analysis. Blood was collected from the carotid arteries, and plasma was separated immediately. Plasma levels of cholesterol, triglycerides, and insulin were measured using commercially available assay kits (Applygen Technologies, Beijing, China). All of the experimental procedures were performed in accordance with protocols approved by the Institutional Animal Care and Research Advisory Committee.



**FIG. 2.** Effect of TM on the insulin signaling pathway in insulin-resistant C2C12 myotubes. **A** and **B**: Protein levels of phosphorylated Akt (p-Akt), total Akt (Akt), phosphorylated AS160 (p-AS160), total AS160 (AS160) (**A**) and plasma membrane protein Glut4 (**B**) in palmitate-free C2C12 myotubes without (control [CON]) or with stimulation of insulin (INS), TM, and insulin (INS) plus TM (INS + TM). C2C12 myotubes treated with palmitate (PA) were stimulated with INS (PA + INS), TM (PA + TM), or INS plus TM (PA + TM + INS). Protein expression was detected by Western blotting. \* $P < 0.05$  and \*\* $P < 0.01$  vs. CON; # $P < 0.05$  vs. PA;  $\Delta P < 0.05$  vs. PA + INS. Data are mean  $\pm$  SEM from 3–6 experiments. **C** and **D**: Protein levels of p-Akt, Akt, p-AS160, AS160 (**C**), and plasma membrane protein Glut4 (**D**) in palmitate-free (CON), only INS (INS), palmitate-treated C2C12 myotubes without (PA) or with stimulation of INS (PA + INS), TM (PA + INS + TM), PPAR $\delta$  inhibitor GSK0660 (GSK, 10  $\mu$ mol/L), PI3K inhibitor LY294002 (LY, 10  $\mu$ mol/L), PPAR $\gamma$  inhibitor GW9662 (GW, 10  $\mu$ mol/L), and PPAR $\alpha$  inhibitor GW6471 (GW6471, 10  $\mu$ mol/L). Protein expression was detected by Western blotting. \* $P < 0.05$  and \*\* $P < 0.01$  vs. CON; # $P < 0.05$  vs. PA + INS;  $\Delta P < 0.05$  vs. PA + INS + TM. Data are mean  $\pm$  SEM from 3–6 experiments.

**IPGTT and IPITT.** IPGTT was performed in mice as previously described (21). After an overnight fast (14 h), glucose (2 g/kg body weight) was administered via injection into the peritoneal cavity, and blood was drawn from the tail vein at 0, 30, 60, and 120 min after glucose administration. Blood glucose levels were determined using the OneTouch Ultra blood glucose meter (LifeScan). IPITT was evaluated in fed mice on a different day. Humulin R (0.75 units/kg body weight; Eli Lilly and Co.) in sterile saline was administered intraperitoneally. Glucose levels were determined at 0, 15, 30, and 60 min after insulin injection. **Acute insulin-stimulation test.** Fasted mice were administered an injection of saline or insulin (5 units/kg of body weight). Gastrocnemius muscles were

collected 5 min after the injection. The phosphorylation of Akt and AS160 was detected by Western blotting in freshly prepared muscle tissue homogenates. Glut4 protein was also detected in plasma membrane homogenates (22).

**Glucose uptake assay.** The glucose uptake assay was conducted as described previously (23), with modifications. Briefly, myotubes were washed with Krebs-Ringer phosphate (KRP) buffer containing 0.05% BSA and incubated at 37°C for 30 min in KRP buffer. Then they were stimulated with insulin in KRP buffer for 10 min at 37°C and were left unstimulated. Cells were further incubated in KRP buffer containing [ $^3$ H]-2-deoxyglucose (1  $\mu$ Ci/mL; PerkinElmer, Boston, MA) in 0.1 mmol/L of unlabeled 2-deoxyglucose for

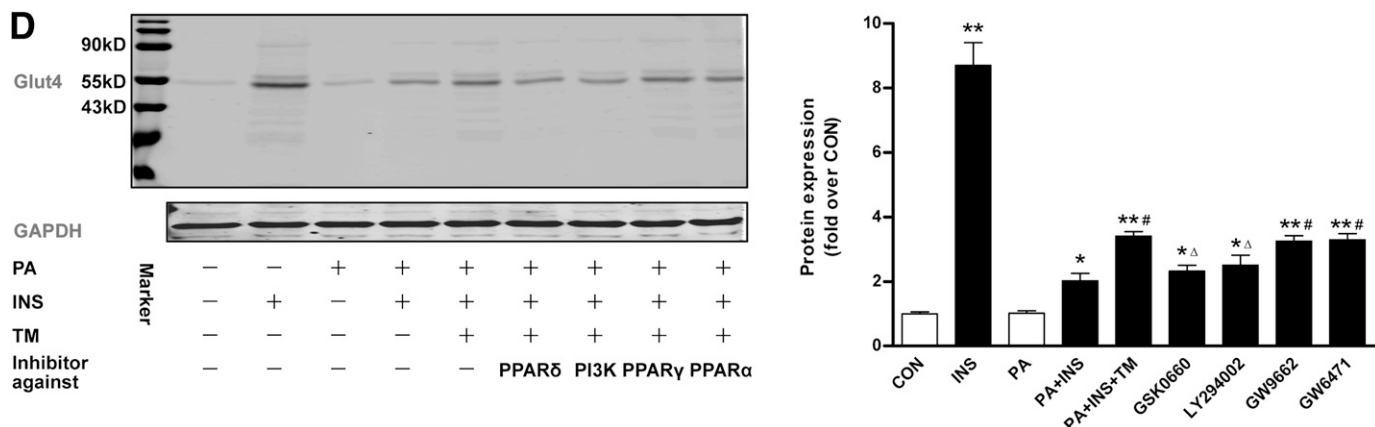


FIG. 2. Continued.

15 min. Cells were washed in ice-cold PBS three times and lysed with 200  $\mu$ L distilled water. A 100- $\mu$ L aliquot of each sample was counted with liquid scintillation, and the rest of the sample was used to determine protein concentration by the Bradford assay. The radioactivity was normalized to the protein concentration.

**C2C12 cell culture and treatment.** Mouse C2C12 myoblasts (ATCC, Manassas, VA) were maintained in Dulbecco's modified Eagle's medium (DMEM; Gibco, Grand Island, NY) with 10% FBS (Gibco) at 37°C in 5% CO<sub>2</sub>/95% O<sub>2</sub> humidified air and differentiated in DMEM with 2% horse serum (Gibco) after reaching confluence. After 4 days, the myoblasts were differentiated into myotubes. Myotubes were incubated with 0.75 mmol/L palmitate for 18 h in DMEM containing 2% BSA and 10% FBS to induce insulin resistance, according to the method described by Wang et al. (24). Cells were then treated with TM dissolved in DMSO (dimethyl sulfoxide, 10  $\mu$ mol/L) or DMSO alone in the presence or absence of indicated inhibitors for 24 h. At the end of treatment, cells were stimulated with 100 nmol/L insulin or PBS for 30 min before total protein or membrane protein were extracted.

**Transfection and luciferase assay.** PPAR responsive element (PPRE) activity was determined by transactivation assays in C2C12 myotubes. Cells were plated in 48-well dishes. Lipofectamine LTX Reagent (Invitrogen, Carlsbad, CA) was used to transfect them with 300 ng luciferase reporter pTK-PPREx3-luc and 150 ng pRL-TK, a renilla luciferase reporter vector as an internal control, with or without cotransfection of 150 ng of the full-length coding region of the rat PPAR $\delta$  expression plasmid pAdTrack-CMV-PPAR $\delta$ , which was generated as described (25). An empty pAdTrack expression vector as the control for PPAR $\delta$  expression vector. After 5 h, transfection medium was replaced by DMEM containing 10% FBS. Cells were then treated with the indicated concentrations of TM in the presence or absence of the indicated inhibitors for an additional 24 h. Cells were assayed for luciferase and renilla activity using the Dual-GloTM Luciferase Assay System (Promega, Madison, WI) and Varioskan Flash Type 3001 (Thermo Electron Corp., Waltham, MA). The luciferase activity was normalized to renilla activity in each sample.

**Western blot analyses.** Western blots of glyceraldehyde-3-phosphate dehydrogenase (GAPDH), PPAR $\delta$ , PPAR $\gamma$ , PPAR $\alpha$ , Akt, phospho-Akt, Akt substrate of 160 kDa (AS160), phospho-AS160, and Glut4 (Santa Cruz Inc., Santa Cruz, CA) were performed as reported (20). The positive control of Glut4 antibody (SC-2243) was provided by Santa Cruz Inc. (Supplementary Data).

**Immunofluorescence.** Immunofluorescence was routinely performed using antibodies against Glut4 (Santa Cruz Inc.). The images were collected using a Nikon TE2000-U inverted fluorescence microscope (Nikon, Tokyo, Japan) and total internal reflection microscopy (Nikon) (26) (Supplementary Data).

**Statistical analyses.** The data are presented as the means  $\pm$  SEM. All analyses were performed with SPSS (version 13.0). Statistical significance of differences between mean values was assessed by Student *t* test or one-way ANOVA with Bonferroni multiple comparison post hoc tests as appropriate. Two-tailed *P* < 0.05 was considered statistically significant.

**RESULTS**

**Effect of TM on PPAR $\delta$  expression and transcriptional activity in C2C12 myotubes.** PPRE activity induced by TM was examined in C2C12 myotubes transfected with a luciferase reporter construct containing three tandem

repeats of PPRE (pTK-PPREx3-luc). In C2C12 myotubes cotransfected with PPAR $\delta$  and pTK-PPREx3-luc, TM induced a time-dependent and dose-dependent enhancement of luciferase activity, which was associated with an upregulation of PPAR $\delta$  protein expression (Fig. 1A and B). PPAR $\delta$  activity and protein expression were slightly changed by acute exposure to TM (15 min or 1 h), whereas PPAR $\delta$  activity and protein expression were significantly increased by chronic TM treatment for 12 h or 24 h (Fig. 1A). TM dose-dependently activated PPAR $\delta$ , but TM at 30  $\mu$ mol/L reduced the PPAR $\delta$  transcriptional activity and protein expression compared with its low doses (Fig. 1B), which could be attributable to the cell toxic effect of high concentration of TM on transcriptional activity (27,28). As shown in Fig. 1C, all three PPAR isoform antagonists significantly inhibited the TM-induced activity. However, the combination of PPAR $\delta$  and PPAR $\gamma$  antagonists (GSK0660 and GW9662) showed no additive effects. Treatment with TM (10  $\mu$ mol/L) significantly increased the luciferase activity and PPAR $\delta$  protein expressions in transfected C2C12 myotubes (Fig. 1D). Furthermore, it showed that incubation with 10  $\mu$ mol/L TM for 24 h significantly upregulated PPAR $\delta$ , PPAR $\gamma$ , and PPAR $\alpha$  expression in C2C12 myotubes (Fig. 1E). These data strongly indicate that TM enhances the expression and transcriptional activity of PPAR $\delta$  in C2C12 myotubes.

**TM improves insulin signaling and glucose uptake through the PPAR $\delta$ /PI3K pathway.** To examine the effect of TM on insulin resistance and its underlying mechanisms, we examined the insulin signaling pathway by measuring Akt, AS160 phosphorylation (29), and plasma membrane Glut4 expression (30) in insulin-sensitive (without palmitate) and palmitate-induced insulin-resistant C2C12 myotubes. In C2C12 myotubes not exposed to palmitate, the phosphorylation of Akt and AS160 and plasma membrane Glut4 expression were increased by  $\sim$ 10-fold after acute insulin stimulation. However, in palmitate-treated insulin-resistant cells, the insulin-induced phosphorylation of Akt and AS160 and plasma membrane Glut4 expression were weak, which could be enhanced by TM treatment. Administration of TM did not restore the phosphorylated Akt or AS160, and it stimulate Glut4 translocation in C2C12 myotubes to the same levels compared with those not exposed to palmitate (Fig. 2A and B). Furthermore, these effects of TM on expression of phospho-Akt, phospho-AS160, and plasma membrane Glut4 were abolished in the presence of either PI3K

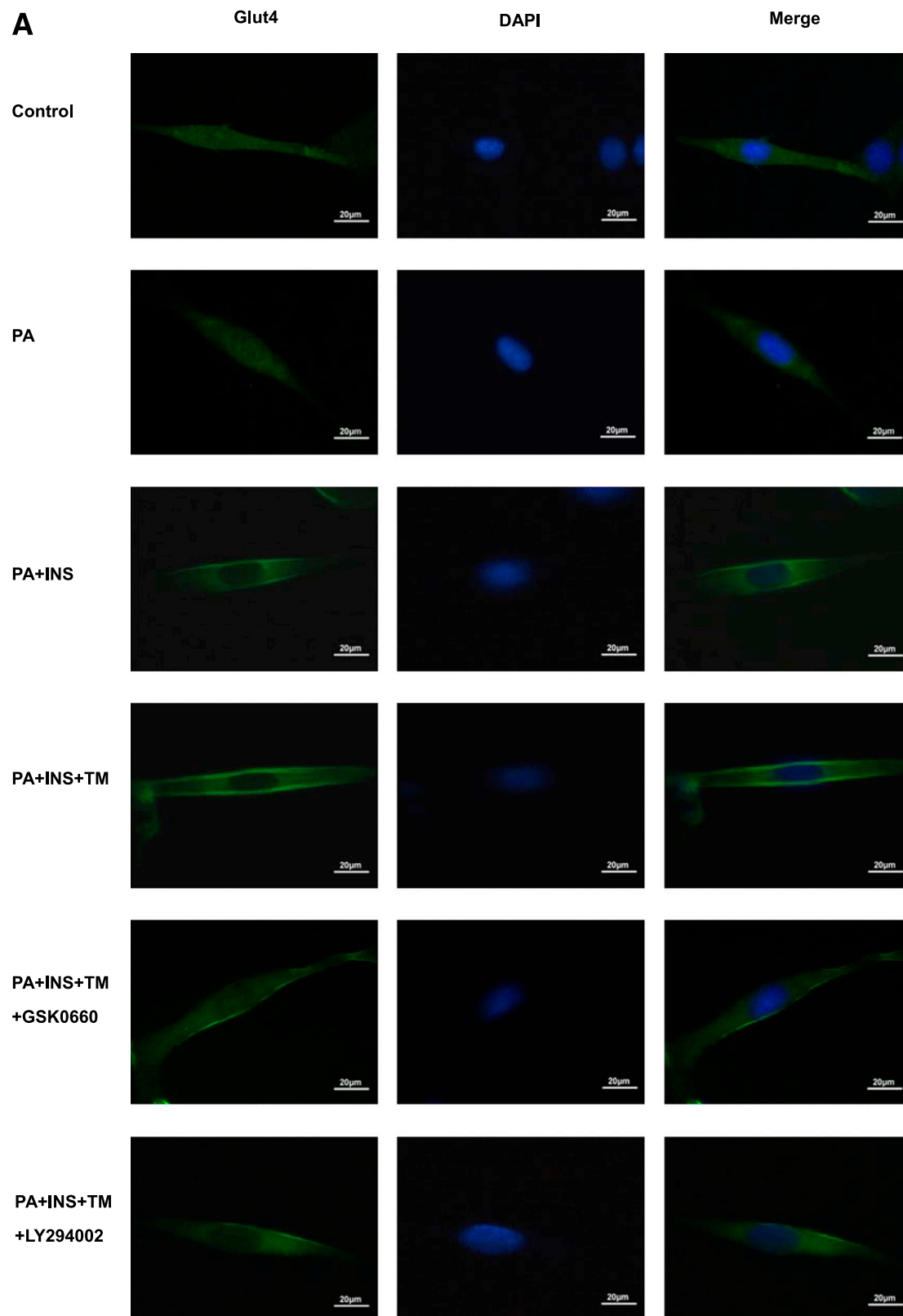


**FIG. 3.** TM effects insulin-stimulated Glut4 translocation and expression and glucose uptake in insulin-resistant C2C12 myotubes. **A** and **B**: TM enhanced insulin-stimulated Glut4 translocation and expression in palmitate-free (control [CON]) and palmitate-treated (PA) C2C12 myotubes, as shown by immunofluorescence, which was attenuated by PPAR $\delta$  and PI3K inhibitors. The green fluorescence indicates Glut4. Nuclei in all groups were stained in blue with DAPI. The images were collected using a Nikon TE2000-U inverted fluorescence microscope (**A**) and total internal reflection microscopy (TIRFM) (**B**). Experiments were repeated three times. **C**: TM increased insulin-stimulated glucose uptake in palmitate-treated C2C12 myotubes. TM did not increase insulin-stimulated glucose uptake without palmitate exposure. The [ $^3$ H]-2-deoxyglucose uptake assays were performed in C2C12 myotubes. \* $P < 0.05$  vs. CON. # $P < 0.05$  vs. insulin [INS]. Data are mean  $\pm$  SEM from six experiments.

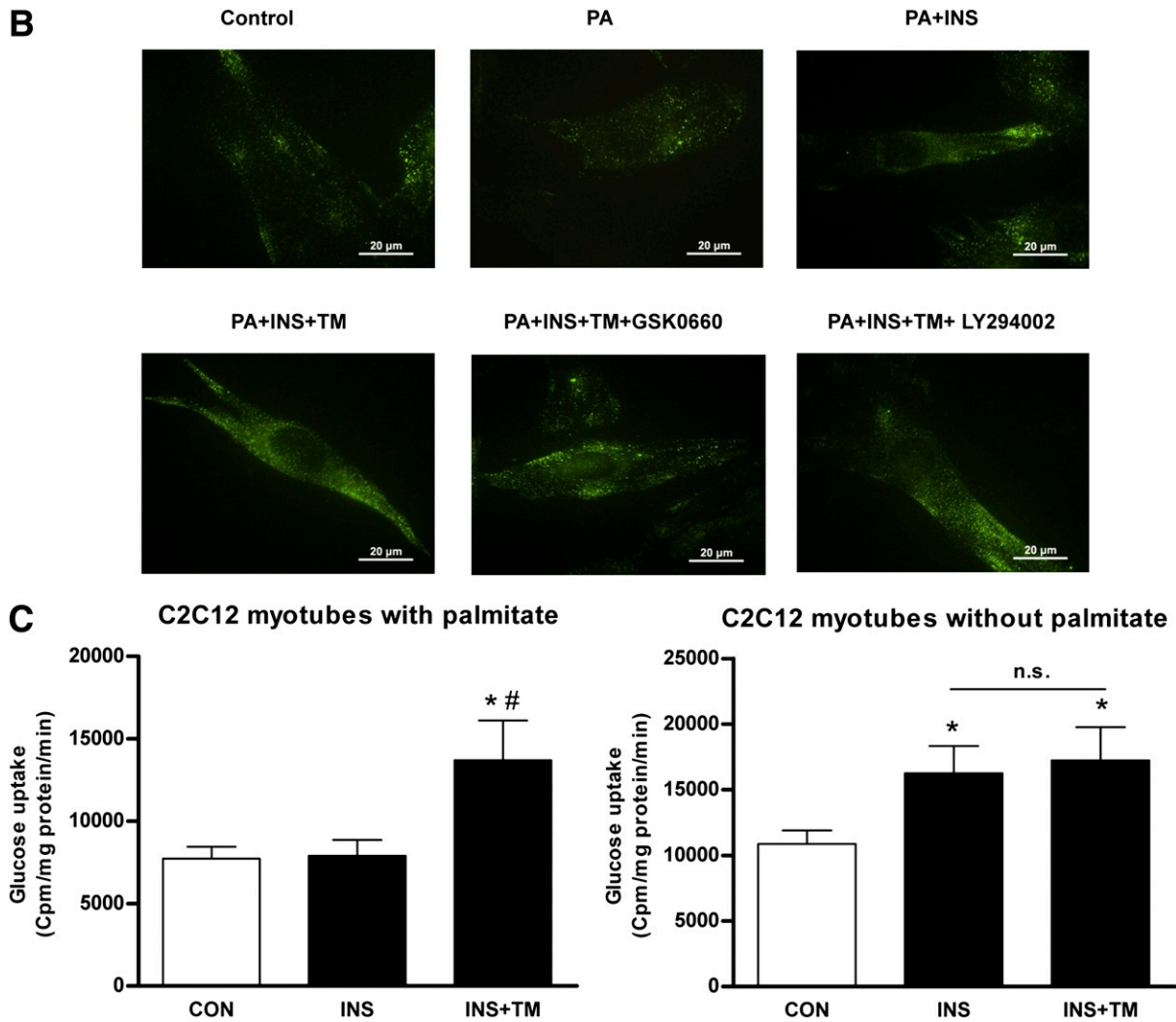


FIG. 3. Continued.

inhibitor LY294002 or PPAR $\delta$  inhibitor GSK0660. However, PPAR $\gamma$  inhibitor GW9662 and PPAR $\alpha$  inhibitor GW6471 did not block the effects of TM (Fig. 2C and D). These results suggest that TM promotes Akt and AS160 phosphorylation and Glut4 translocation in insulin-resistant C2C12 myotubes in a PPAR $\delta$ /PI3K-dependent, but not in a PPAR $\gamma$ -dependent or PPAR $\alpha$ -dependent, manner.

It is well-known that insulin stimulation induces Glut4 translocation to the cellular membrane and thus facilitates glucose uptake in skeletal muscle (30–32). In palmitate-induced insulin-resistant C2C12 myotubes, insulin had little effect on Glut4 translocation to the membrane, as shown by immunofluorescence (Fig. 3A and B). However, cotreatment with TM markedly enhanced the insulin-stimulated Glut4 translocation and expression, and this effect was attenuated in the presence of PPAR $\delta$  inhibitor or PI3K inhibitor (Fig. 3A and B). We further examined the glucose uptake in C2C12 and palmitate-treated primary cultured myotubes from mice. Insulin stimulation significantly increased in glucose uptake of cells without palmitate treatment but had little effect on myotubes with palmitate (Fig. 3C and Supplementary Fig. 1). TM significantly increased the insulin-stimulated glucose uptake in C2C12

and mice myotubes in the presence of palmitate (Fig. 3C and Supplementary Fig. 1A).

**TM treatment reverses insulin resistance of skeletal muscle in mice.** To verify the effect of TM on glucose homeostasis in vivo, we first established insulin resistance in mice fed a HFD for 20 weeks. The glucose tolerance and insulin sensitivity were both significantly impaired in HFD-fed mice, as detected by IPGTT and IPITT, respectively (Supplementary Fig. 2A and B). Next, these insulin-resistant mice were randomly divided into HF group and HF plus TM group for another 10 weeks. Both glucose tolerance and insulin sensitivity in the HF plus TM group were significantly improved, whereas those in the HF group were still significantly impaired compared with control mice fed a regular diet. However, neither the glucose intolerance nor the insulin resistance was improved in MCK-PPAR $\delta$ <sup>-/-</sup> mice fed the HFD plus TM (Fig. 4A and B).

Mice fed a HFD had higher levels of plasma insulin, triglycerides, and cholesterol compared with the control mice fed the regular diet. TM significantly reduced these elevations of blood parameters in WT mice fed a HFD (Fig. 5A and B). In addition, chronic TM treatment prevented HFD-induced obesity in WT mice (Fig. 5C). The average food intake was similar between all groups of mice (Fig. 5D). Taken

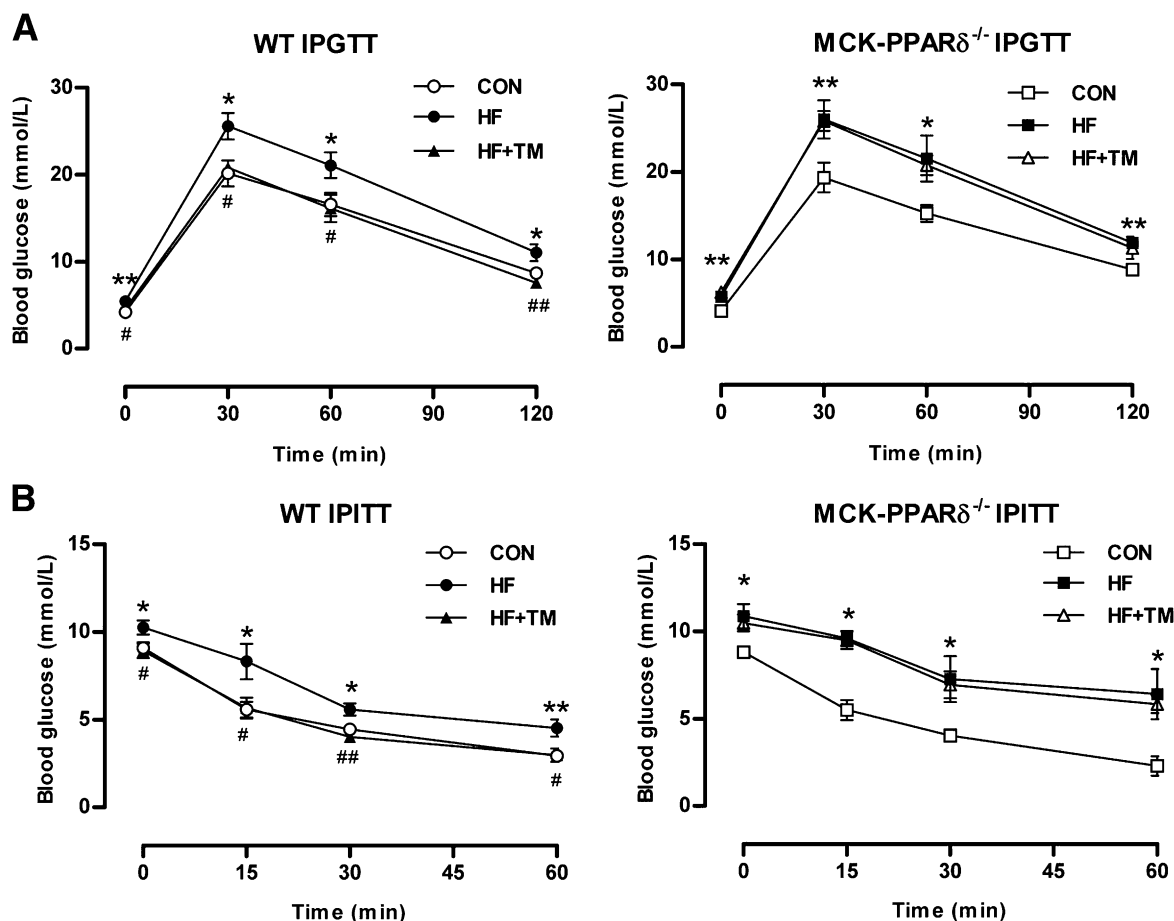


FIG. 4. Effect of TM treatment on HFD-induced insulin resistance and glucose intolerance in mice. *A* and *B*: Glucose tolerance (*A*) and insulin tolerance (*B*) were measured by IPGTT and IPITT, respectively, in WT and MCK-PPAR $\delta^{-/-}$  mice with or without TM treatment for 10 weeks. CON, mice fed chow diet; HF, mice fed HFD for 20 weeks and continuing for the next 10 weeks; HF+TM, mice fed HFD for 20 weeks and then HFD plus TM for 10 weeks. \* $P < 0.05$  and \*\* $P < 0.01$  vs. CON; # $P < 0.05$  and ## $P < 0.01$  vs. HF. Data are mean  $\pm$  SEM ( $n = 6$  for each group).

together, these findings indicate that long-term TM treatment significantly attenuates HFD-induced insulin resistance, hyperinsulinemia, hyperlipidemia, and obesity through stimulation of PPAR $\delta$  activity and protein expression.

**Chronic TM treatment enhances PPAR $\delta$ -mediated insulin signaling proteins and Glut4 in skeletal muscle.** To further investigate the underlying mechanism of TM action in vivo, we detected the protein expression of PPAR $\delta$ , PPAR $\gamma$ , PPAR $\alpha$ , and insulin-signaling proteins in the gastrocnemius muscle tissue of WT and MCK-PPAR $\delta^{-/-}$  mice with or without acute insulin stimulation. As shown in Fig. 6*A* and *C*, WT mice fed a HFD had a significantly lower PPAR $\delta$  level in skeletal muscle, whereas this reduction of PPAR $\delta$  was markedly reversed by TM treatment for 10 weeks. However, the expressions of PPAR $\gamma$  and PPAR $\alpha$  were slightly increased by TM compared with HFD group in WT and MCK-PPAR $\delta^{-/-}$  mice (Fig. 6*A* and *B*). Furthermore, the protein levels of phospho-Akt, phospho-AS160, and plasma membrane Glut4 in skeletal muscle were significantly decreased in HFD-fed mice, which were significantly increased by chronic TM treatment in WT mice but not in MCK-PPAR $\delta^{-/-}$  mice (Fig. 6*C–F*). This in vivo evidence indicates that long-term TM treatment enhances Akt and AS160 phosphorylation and Glut4 translocation through PPAR $\delta$  activation, which could be responsible for the insulin-sensitizing effects of TM in skeletal muscle.

## DISCUSSION

The current study demonstrates that TM can improve insulin sensitivity and increase insulin-stimulated glucose uptake in both cultured myotubes and skeletal muscle from mice. Importantly, this effect was PPAR $\delta$ -dependent, because the genetic deletion of PPAR $\delta$  and the presence of PPAR $\delta$  antagonist abolished the insulin-sensitizing effect of TM. Furthermore, the beneficial effect of TM on glucose homeostasis is associated with increased phosphorylation of Akt and AS160, and Glut4 translocation, which were absent in MCK-PPAR $\delta$  knockout mice. Thus, in addition to previously reported effects on PPAR $\gamma$  activation, we show for the first time that TM enhances glucose uptake and insulin sensitivity through activation of PPAR $\delta$ -mediated PI3K signaling in skeletal muscle.

Most hypertensive patients are insulin resistant, and the risk of cardiovascular events is remarkably higher when complicated with diabetes (1,2). Several clinical trials have demonstrated that angiotensin-converting enzyme inhibitors and ARBs may prevent the new onset of diabetes in patients with hypertension (3). Mori et al. (33) and de Luis et al. (34) reported TM improves insulin sensitivity in patients with obesity-related hypertension. Krämer et al. (11) showed that activation of PPAR $\delta$  results in a direct increase of fatty acid transport and glucose uptake and

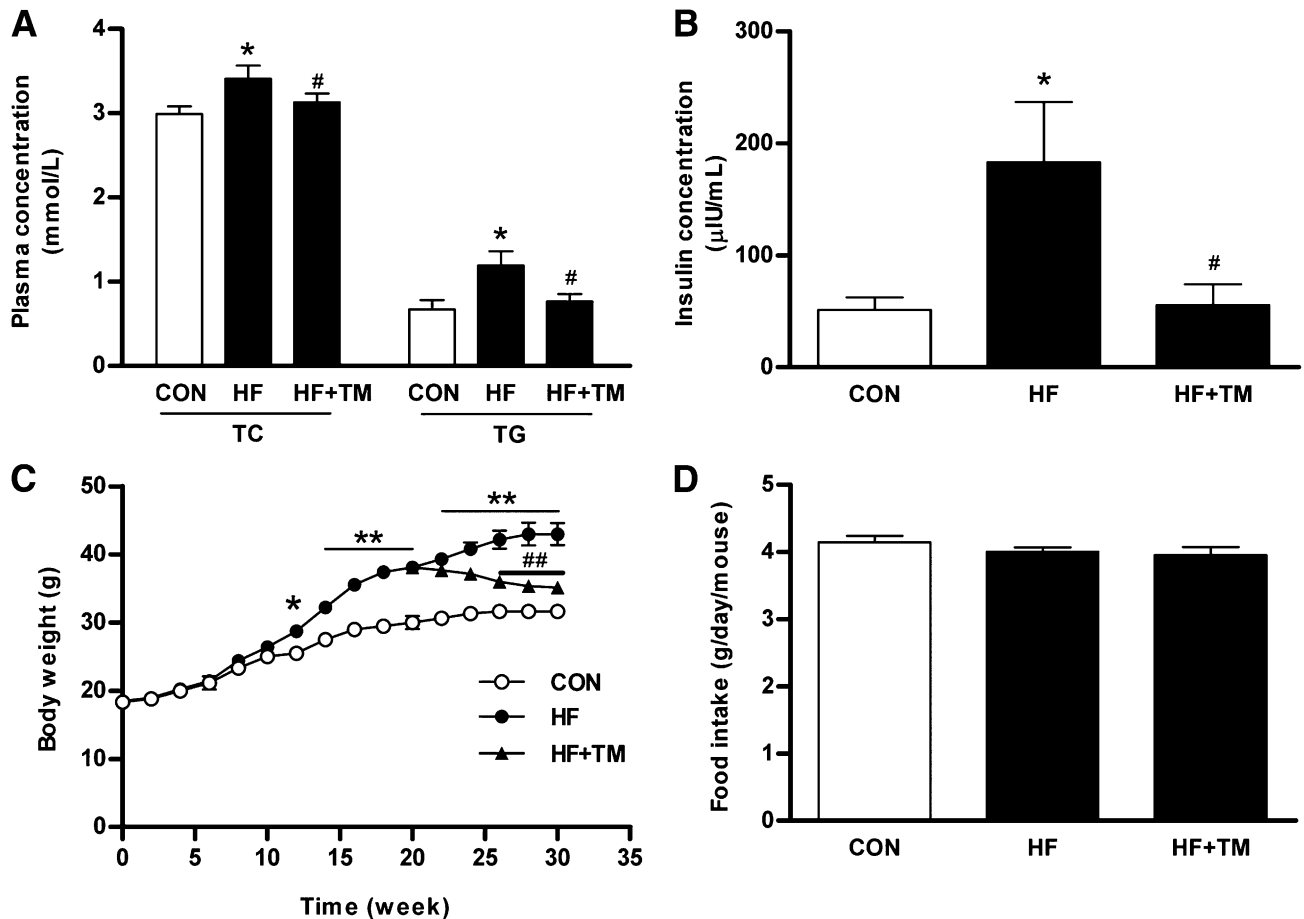


**FIG. 5.** Effect of TM treatment on the blood parameters, body weight, and food intake in mice. **A:** Plasma levels of total cholesterol (TC) and triglycerides (TG) in WT mice. **B:** Plasma levels of insulin in WT mice. Mice were killed after fasting for 14 h. The blood was collected from the carotid artery, and plasma was separated within 1 h. These parameters were examined within 24 h using commercially available kits. **C:** Time-dependent changes in body weight of the mice throughout the intervention. **D:** Average daily food intake per mouse in the second week of the intervention. \* $P < 0.05$  and \*\* $P < 0.01$  vs. control (CON); # $P < 0.05$  and ## $P < 0.01$  vs. HF. Data are mean  $\pm$  SEM ( $n = 6$  for each group).

promotes lipid and glucose metabolism and gene expression in primary cultured human skeletal muscle cells. At 40 mg TM and 160 mg TM, the bioavailability was 42% and 58%, respectively, in humans. Maximal concentrations of TM in human plasma were  $159 \pm 104$  ng/mL for 40 mg and  $693 \pm 606$  ng/mL for 80 mg (35). Plasma concentration was  $142.86 \pm 14.85$  ng/mL in adult C57BL/6J male mice after 1 mg/kg per day administration of TM for 7 days (36). In this study, we treated adult C57BL/6J mice with TM (5 mg/kg per day) for the long-term (37).

The underlying mechanisms of TM that improve insulin sensitivity are not fully elucidated. Previous studies show that TM can increase adiponectin levels, which improves insulin sensitivity (5). Additionally, other beneficial effects of ARBs were reported, including improvement of microcirculation in skeletal muscle (4), reduction of body weight (38), protection of pancreatic islets from glucotoxicity, and oxidative impairment (39). In particular, some ARBs, including TM, can act as a partial agonist of PPAR $\gamma$  (40). Activation of PPAR $\gamma$  consequently might facilitate insulin signaling and improve insulin secretion in  $\beta$  cells (41).

Clemenz et al. (42) recently found that TM also acts as a partial PPAR $\alpha$  agonist, at least in the liver, indicating that the various actions of TM might include activation of different PPAR subtypes. Compared with PPAR $\gamma$ , which is rarely expressed in skeletal muscle, PPAR $\delta$  is highly

expressed in skeletal muscle (10). PPAR $\delta$  activation in adipose tissue leads to enhanced fatty acid oxidation, improved lipid profile, and increased CB1 expression (25), as well as improved glucose metabolism (43). PPAR $\delta$  activation in cultured human skeletal muscle cells promotes gene-regulatory responses (11). Muscle-specific PPAR $\delta$  overexpression results in a profound remodeling of myofibers attributable to hyperplasia and a shift to more oxidative fibers, and it increases both the activity and the expression of enzymes involved in oxidative metabolism (12,16).

It was unknown whether TM had an effect on PPAR $\delta$ . Our study shows that TM acts through PPAR $\delta$  in skeletal muscle. First, we demonstrated that TM activates PPAR $\delta$  transcriptional activity and upregulates PPAR $\delta$  expression in C2C12 myotubes. Second, long-term administration of TM markedly increases PPAR $\delta$  expression in the skeletal muscle from insulin-resistant mice. Third, no TM stimulatory effect is observed in skeletal muscle from MCK-PPAR $\delta$  knockout mice or myotubes in the presence of a PPAR $\delta$  antagonist. These observations support the notion that TM activates PPAR $\delta$  in skeletal muscle. Skeletal muscle is one of the major insulin target tissues responsible for the maintenance of whole-body glucose homeostasis and accounts for the bulk of insulin-stimulated glucose utilization (30). Glucose transport in skeletal

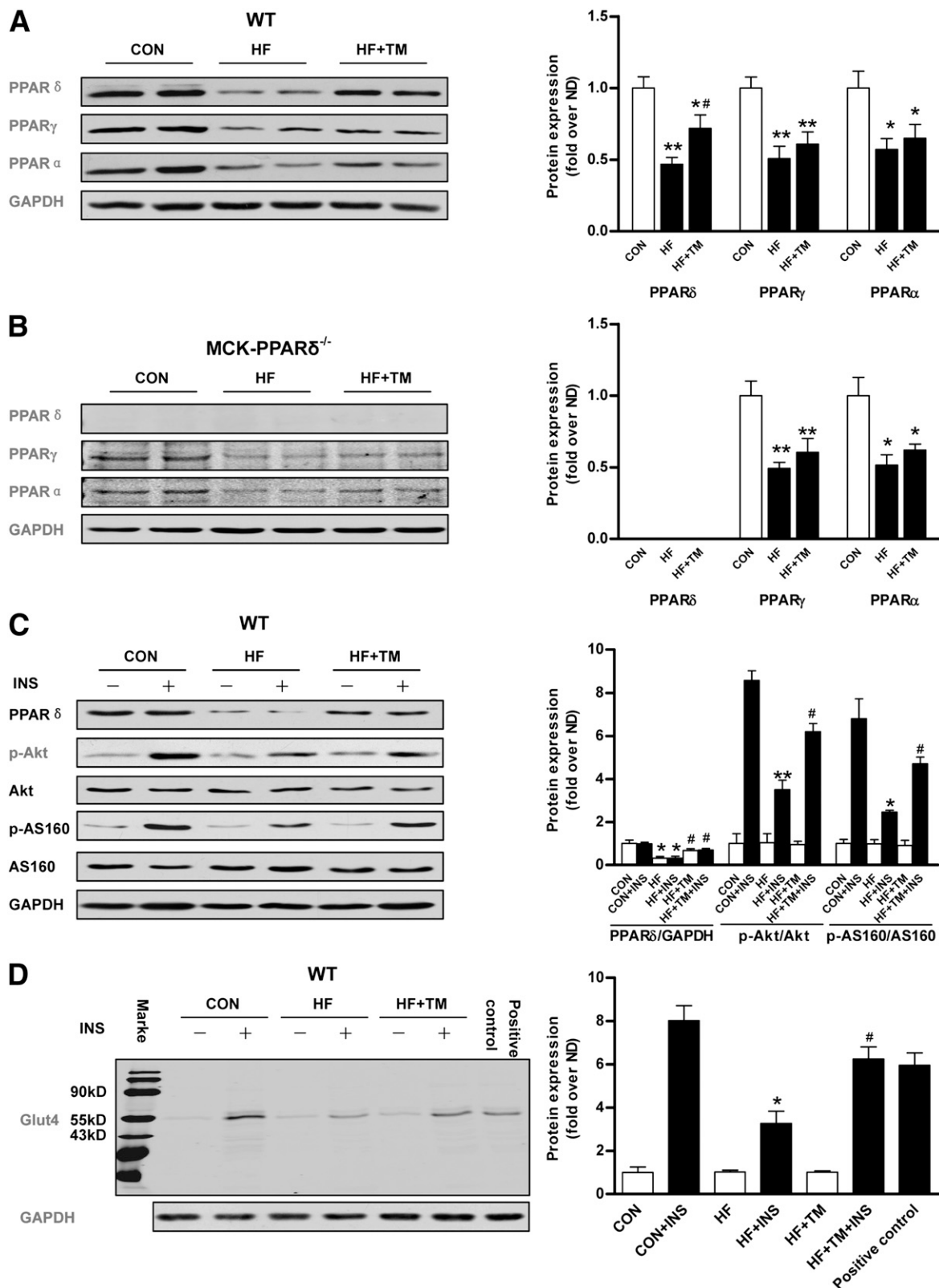


**FIG. 6.** Effects of TM on PPAR $\delta$ , phospho-Akt, phospho-AS160, and Glut4 protein levels in skeletal muscle of mice. *A* and *B*: Protein levels of PPAR $\delta$ , PPAR $\gamma$ , and PPAR $\alpha$  in WT (*A*) and MCK-PPAR $\delta^{-/-}$  (*B*) mice were detected by Western blotting. \* $P < 0.05$  and \*\* $P < 0.01$  vs. control (CON); # $P < 0.05$  vs. HF ( $n = 3-6$  for each group). *C* and *D*: Protein levels and bar graph of PPAR $\delta$ , p-Akt, Akt, p-AS160, AS160 (*C*), and plasma membrane Glut4 (*D*) in skeletal muscle of WT mice as detected by Western blotting with or without acute insulin stimulation. *E* and *F*: Protein levels and bar graph of PPAR $\delta$ , p-Akt, Akt, p-AS160, AS160 (*E*), and plasma membrane Glut4 (*F*) in skeletal muscle of MCK-PPAR $\delta^{-/-}$  mice as detected by Western blotting with or without acute insulin-stimulation. \* $P < 0.05$  and \*\* $P < 0.01$  vs. CON plus insulin (CON+INS); # $P < 0.05$  vs. HF+INS ( $n = 3-6$  for each group).

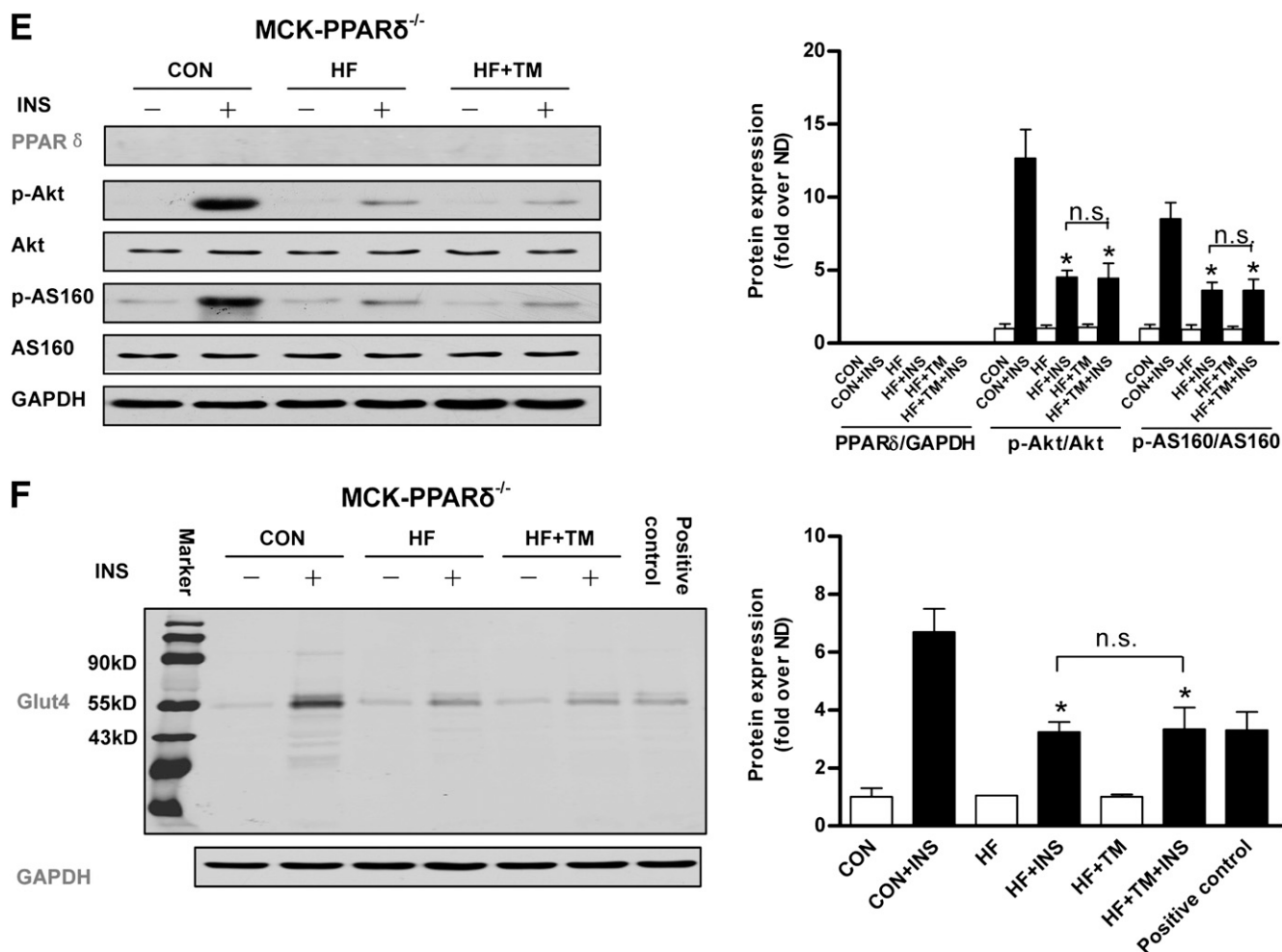


FIG. 6. Continued.

muscle is mainly regulated by glucose transporter Glut4 (30). Insulin stimulates glucose uptake by recruiting Glut4 from an intracellular pool to the cell surface through a mechanism that is dependent on PI3K (30). Insulin resistance leads to defective PI3K/Akt signaling, reduced Glut4 expression, and impaired insulin-stimulated glucose uptake (30). The activation of the PI3K/Akt pathway by PPAR $\delta$  agonists has been reported previously in several cell types, such as hepatocytes, epithelial cells, and lung cancer cell lines (44–46). In addition, PPAR $\delta$  agonists also are reported to increase glucose uptake in an insulin-independent manner and lead to the phosphorylation of AMP-activated protein kinase and p38 mitogen-activated protein kinase in cultured primary human skeletal muscle cells (47).

Against this background, we examined the effect of TM on glucose transport and its underlying mechanism in the skeletal muscle. First, using a common *in vitro* cell model for insulin resistance, we first showed that TM enhanced insulin-stimulated glucose uptake in cultured myotubes. Second, TM promoted the insulin-stimulated translocation of Glut4 in cultured C2C12 myotubes. Third, TM increased phospho-Akt, phospho-AS160, and plasma membrane Glut4 expression in the presence of insulin; however, this effect was inhibited by a PPAR $\delta$  antagonist and a PI3K inhibitor, but not by PPAR $\gamma$  and PPAR $\alpha$  antagonists in cultured myotubes. Experimental evidences *in vivo* further

showed that WT mice fed a HFD and development of glucose intolerance and insulin resistance. Chronic TM treatment reversed the HFD-induced insulin resistance and glucose intolerance in WT mice but not in MCK-PPAR $\delta$ <sup>-/-</sup> mice. Meanwhile, TM treatment promoted phosphorylation of Akt and AS160, and increased the expression of PPAR $\delta$  and plasma membrane Glut4 in the skeletal muscle of WT mice but not in MCK-PPAR $\delta$ <sup>-/-</sup> mice.

These findings strongly imply a previously unrecognized role for TM in promoting glucose uptake and improving insulin sensitivity through activation of the PPAR $\delta$ /PI3K pathway, which may have additional benefits during diabetes therapy. However, TM is not able to eliminate the insulin resistance induced; it only partly improves the defects induced by palmitate. Although TM treatment can increase insulin sensitivity through activation of PPAR $\delta$ /PI3K pathway in insulin-resistant myotubes induced by palmitate and in mice fed a HFD, the pathophysiology of human diabetes is somewhat different from that obtained in rodents. Further studies are worthy to clarify this point. From a clinical perspective, our findings highlight an important role for TM in the improvement of insulin resistance in the skeletal muscle and further implicate PPAR $\delta$  as a potential therapeutic target in the treatment of hypertensive subjects with type 2 diabetes.

In summary, we demonstrate that TM has a profound role in the improvement of glucose homeostasis in skeletal

muscle, which is associated with activation of the PPAR $\delta$ /PI3K pathway. It is tempting to speculate that our data provide the molecular basis for the use of ARBs in the treatment and prevention of diabetes in hypertensive patients. A randomized clinical trial is needed to verify whether ARBs could provide additional improvements of skeletal muscle function to hypertensive patients.

#### ACKNOWLEDGMENTS

This study was funded by the Natural Science Foundation of China (grant no. 30890042) and by National Basic Research Program (973 Program) grants from China (grant no. 2012CB517806 and 2011CB503902).

No potential conflicts of interest relevant to this article were reported.

L.L. and Z.L. performed most of the experiments, analyzed data, and wrote the manuscript. H.Y. performed some experiments and contributed to the discussion. X.F. reviewed and edited the manuscript. P.W., J.C., Y.P., Y.Z., H.H., and J.Z. performed some experiments. D.L. contributed to the discussion and edited the manuscript. Z.Z. designed the experiments and wrote and edited the manuscript. Z.Z. is the guarantor of this work and, as such, had full access to all of the data in the study and takes responsibility for the integrity of the data and the accuracy of the data analysis.

The authors thank Tingbing Cao and Lijuan Wang (Chongqing Institute of Hypertension, China) for technical assistance. The authors thank Bin Tan (Institute of Pediatrics, Children's Hospital of Chongqing Medical University) for immunofluorescence images from total internal reflection microscopy. The authors thank Prof. Yu Huang and Dr. Wing Tak Wong (Chinese University of Hong Kong, China) for critical review of the manuscript.

#### REFERENCES

- Taylor R. Insulin resistance and type 2 diabetes. *Diabetes* 2012;61:778–779
- Putnam K, Shoemaker R, Yiannikouris F, Cassis LA. The renin-angiotensin system: a target of and contributor to dyslipidemias, altered glucose homeostasis, and hypertension of the metabolic syndrome. *Am J Physiol Heart Circ Physiol* 2012;302:H1219–H1230
- McMurray JJ, Holman RR, Haffner SM, et al.; NAVIGATOR Study Group. Effect of valsartan on the incidence of diabetes and cardiovascular events. *N Engl J Med* 2010;362:1477–1490
- Chai W, Wang W, Liu J, et al. Angiotensin II type 1 and type 2 receptors regulate basal skeletal muscle microvascular volume and glucose use. *Hypertension* 2010;55:523–530
- Furuhashi M, Ura N, Higashiura K, et al. Blockade of the renin-angiotensin system increases adiponectin concentrations in patients with essential hypertension. *Hypertension* 2003;42:76–81
- Schupp M, Clemenz M, Gineste R, et al. Molecular characterization of new selective peroxisome proliferator-activated receptor  $\gamma$  modulators with angiotensin receptor blocking activity. *Diabetes* 2005;54:3442–3452
- Benson SC, Pershadsingh HA, Ho CI, et al. Identification of telmisartan as a unique angiotensin II receptor antagonist with selective PPAR $\gamma$  modulating activity. *Hypertension* 2004;43:993–1002
- Spiegelman BM. PPAR- $\gamma$ : adipogenic regulator and thiazolidinedione receptor. *Diabetes* 1998;47:507–514
- Grimaldi B, Bellet MM, Katada S, et al. PER2 controls lipid metabolism by direct regulation of PPAR $\gamma$ . *Cell Metab* 2010;12:509–520
- Ehrenborg E, Krook A. Regulation of skeletal muscle physiology and metabolism by peroxisome proliferator-activated receptor delta. *Pharmacol Rev* 2009;61:373–393
- Krämer DK, Al-Khalili L, Guigas B, Leng Y, Garcia-Roves PM, Krook A. Role of AMP kinase and PPAR $\delta$  in the regulation of lipid and glucose metabolism in human skeletal muscle. *J Biol Chem* 2007;282:19313–19320
- Luquet S, Lopez-Soriano J, Holst D, et al. Peroxisome proliferator-activated receptor delta controls muscle development and oxidative capability. *FASEB J* 2003;17:2299–2301
- Gan Z, Burkart-Hartman EM, Han DH, et al. The nuclear receptor PPAR $\beta$ / $\delta$  programs muscle glucose metabolism in cooperation with AMPK and MEF2. *Genes Dev* 2011;25:2619–2630
- Schuler M, Ali F, Chambon C, et al. PGC1 $\alpha$  expression is controlled in skeletal muscles by PPAR $\beta$ , whose ablation results in fiber-type switching, obesity, and type 2 diabetes. *Cell Metab* 2006;4:407–414
- Lee CH, Olson P, Hevener A, et al. PPAR $\delta$  regulates glucose metabolism and insulin sensitivity. *Proc Natl Acad Sci USA* 2006;103:3444–3449
- Wang YX, Zhang CL, Yu RT, et al. Regulation of muscle fiber type and running endurance by PPAR $\delta$ . *PLoS Biol* 2004;2:e294
- Harman FS, Nicol CJ, Marin HE, Ward JM, Gonzalez FJ, Peters JM. Peroxisome proliferator-activated receptor-delta attenuates colon carcinogenesis. *Nat Med* 2004;10:481–483
- Gupta RA, Wang D, Katkuri S, Wang H, Dey SK, DuBois RN. Activation of nuclear hormone receptor peroxisome proliferator-activated receptor-delta accelerates intestinal adenoma growth. *Nat Med* 2004;10:245–247
- Brüning JC, Michael MD, Winnay JN, et al. A muscle-specific insulin receptor knockout exhibits features of the metabolic syndrome of NIDDM without altering glucose tolerance. *Mol Cell* 1998;2:559–569
- Zhang LL, Yan Liu D, Ma LQ, et al. Activation of transient receptor potential vanilloid type-1 channel prevents adipogenesis and obesity. *Circ Res* 2007;100:1063–1070
- Ma S, Yu H, Zhao Z, et al. Activation of the cold-sensing TRPM8 channel triggers UCP1-dependent thermogenesis and prevents obesity. *J Mol Cell Biol* 2012;4:88–96
- McClung JP, Roneker CA, Mu W, et al. Development of insulin resistance and obesity in mice overexpressing cellular glutathione peroxidase. *Proc Natl Acad Sci USA* 2004;101:8852–8857
- Merlin J, Evans BA, Csikasz RI, Bengtsson T, Summers RJ, Hutchinson DS. The M3-muscarinic acetylcholine receptor stimulates glucose uptake in L6 skeletal muscle cells by a CaMKK-AMPK-dependent mechanism. *Cell Signal* 2010;22:1104–1113
- Wang X, Yu W, Nawaz A, Guan F, Sun S, Wang C. Palmitate induced insulin resistance by PKC $\theta$ -dependent activation of mTOR/S6K pathway in C2C12 myotubes. *Exp Clin Endocrinol Diabetes* 2010;118:657–661
- Yan ZC, Liu DY, Zhang LL, et al. Exercise reduces adipose tissue via cannabinoid receptor type 1 which is regulated by peroxisome proliferator-activated receptor-delta. *Biochem Biophys Res Commun* 2007;354:427–433
- Levskaia A, Weiner OD, Lim WA, Voigt CA. Spatiotemporal control of cell signalling using a light-switchable protein interaction. *Nature* 2009;461:997–1001
- Yamamoto K, Ohishi M, Ho C, Kurtz TW, Rakugi H. Telmisartan-induced inhibition of vascular cell proliferation beyond angiotensin receptor blockade and peroxisome proliferator-activated receptor-gamma activation. *Hypertension* 2009;54:1353–1359
- Tagami T, Yamamoto H, Moriyama K, et al. A selective peroxisome proliferator-activated receptor-gamma modulator, telmisartan, binds to the receptor in a different fashion from thiazolidinediones. *Endocrinology* 2009;150:862–870
- Alkhateeb H, Chabowski A, Glatz JF, Gurd B, Luiken JJ, Bonen A. Restoring AS160 phosphorylation rescues skeletal muscle insulin resistance and fatty acid oxidation while not reducing intramuscular lipids. *Am J Physiol Endocrinol Metab* 2009;297:E1056–E1066
- Leto D, Saltiel AR. Regulation of glucose transport by insulin: traffic control of GLUT4. *Nat Rev Mol Cell Biol* 2012;13:383–396
- Xie X, Gong Z, Mansuy-Aubert V, et al. C2 domain-containing phosphoprotein CDP138 regulates GLUT4 insertion into the plasma membrane. *Cell Metab* 2011;14:378–389
- Yip MF, Ramm G, Larance M, et al. CaMKII-mediated phosphorylation of the myosin motor Myo1c is required for insulin-stimulated GLUT4 translocation in adipocytes. *Cell Metab* 2008;8:384–398
- Mori Y, Tanaka T, Matsuura K, Yokoyama J, Utsunomiya K. Influence of telmisartan on insulin response after glucose loading in obese patients with hypertension: ARB trial of hypertension in obese patients with hyperinsulinemia assessed by oral glucose tolerance test (ATHLETE). *Adv Ther* 2011;28:698–706
- de Luis DA, Conde R, González-Sagrado M, et al. Effects of telmisartan vs olmesartan on metabolic parameters, insulin resistance and adipocytokines in hypertensive obese patients. *Nutr Hosp* 2010;25:275–279
- Smith DH, Matzek KM, Kempthorne-Rawson J. Dose response and safety of telmisartan in patients with mild to moderate hypertension. *J Clin Pharmacol* 2000;40:1380–1390
- Washida K, Ihara M, Nishio K, et al. Nonhypotensive dose of telmisartan attenuates cognitive impairment partially due to peroxisome proliferator-

- activated receptor-gamma activation in mice with chronic cerebral hypoperfusion. *Stroke* 2010;41:1798–1806
37. Araki K, Masaki T, Katsuragi I, Tanaka K, Kakuma T, Yoshimatsu H. Telmisartan prevents obesity and increases the expression of uncoupling protein 1 in diet-induced obese mice. *Hypertension* 2006;48:51–57
  38. He H, Yang D, Ma L, et al. Telmisartan prevents weight gain and obesity through activation of peroxisome proliferator-activated receptor-delta-dependent pathways. *Hypertension* 2010;55:869–879
  39. Tikellis C, Cooper ME, Thomas MC. Role of the renin-angiotensin system in the endocrine pancreas: implications for the development of diabetes. *Int J Biochem Cell Biol* 2006;38:737–751
  40. Yuen CY, Wong WT, Tian XY, et al. Telmisartan inhibits vasoconstriction via PPAR $\gamma$ -dependent expression and activation of endothelial nitric oxide synthase. *Cardiovasc Res* 2011;90:122–129
  41. Brunham LR, Kruit JK, Pape TD, et al. Beta-cell ABCA1 influences insulin secretion, glucose homeostasis and response to thiazolidinedione treatment. *Nat Med* 2007;13:340–347
  42. Clemenz M, Frost N, Schupp M, et al. Liver-specific peroxisome proliferator-activated receptor  $\alpha$  target gene regulation by the angiotensin type 1 receptor blocker telmisartan. *Diabetes* 2008;57:1405–1413
  43. Kang K, Reilly SM, Karabacak V, et al. Adipocyte-derived Th2 cytokines and myeloid PPARdelta regulate macrophage polarization and insulin sensitivity. *Cell Metab* 2008;7:485–495
  44. Pang M, de la Monte SM, Longato L, et al. PPARdelta agonist attenuates alcohol-induced hepatic insulin resistance and improves liver injury and repair. *J Hepatol* 2009;50:1192–1201
  45. Jimenez R, Sanchez M, Zarzuelo MJ, et al. Endothelium-dependent vasodilator effects of peroxisome proliferator-activated receptor beta agonists via the phosphatidylinositol-3 kinase-Akt pathway. *J Pharmacol Exp Ther* 2010;332:554–561
  46. Pedchenko TV, Gonzalez AL, Wang D, DuBois RN, Massion PP. Peroxisome proliferator-activated receptor beta/delta expression and activation in lung cancer. *Am J Respir Cell Mol Biol* 2008;39:689–696
  47. Krämer DK, Al-Khalili L, Perrini S, et al. Direct activation of glucose transport in primary human myotubes after activation of peroxisome proliferator-activated receptor  $\delta$ . *Diabetes* 2005;54:1157–1163